Applied Thermal Engineering 141 (2018) 579–588

Contents lists available at ScienceDirect

Applied Thermal Engineering

journal homepage: www.elsevier.com/locate/apthermeng

Research Paper

Photon application in the design of sustainable buildings to console global energy and environment

Md. Faruque Hossain*

Department of Civil and Urban Engineering, New York University, 6 Metrotech Center, Brooklyn, NY 11201, USA
Green Globe Technology, 4323 Colden Street 15L, Flushing, NY 11355, USA

HIGHLIGHTS

- Building curtain wall has been utilized as PV panel to capture solar energy.
- Photon has been clarified by PV panel to convert into electricity energy.
- Energy production was calculated to meet the energy need for a building.

ARTICLE INFO

Keywords:
Global environmental vulnerability
Solar radiation
PV panel acting build skin
Clean energy production
Climate change mitigation

ABSTRACT

Photon energy has been implemented to design the sustainable building where at least 25% of its exterior curtain skin wall could be used as the acting Photovoltaics (PV) panel to trap the solar energy to transform into electricity to satisfy energy demand for a building itself without any outsource connection. Given the current rate of conventional fuel consumption, atmospheric greenhouse gas emission (GHGs) increasing rapidly where building sector along responsible for 40% GHGs emission. These GHGs ultimately causing environmental vulnerability such as climate change, stratospheric ozone depletion, acid rain, flooding, and air toxicity which threatening to survive all living being on Earth. Therefore, the mechanism of photophysical transformation by the acting PV panel of the building exterior skin in response to solar radiation shall indeed would be a cutting-edge technology to console the global energy demand and mitigate the climate change perplexity dramatically.

1. Introduction

Massive development of conventional urbanization throughout the world is consuming fossil energy tremendously. Consequently, it is causing severe environmental perplexity such as acid deposition, stratospheric ozone depletion, and climate change severely where traditional building development along responsible for 40% of this environmental and climate change disaster [2,3,51]. Besides, conventional energy deposition is getting finite level. At present the total amount of fossil fuel reserved in the whole world is 36,600 EJ (crude oil 1.65 × 1011 t or unit energy 4.2×10^{10} J/t is equivalent to 6930 EJ; natural gas 1.81×10^{14} t or unit energy 3.6×107 J/m^3 is equivalent to 6500 EJ; high-quality coal 4.90×10^{11} t or unit energy 3.1×10^{10} J/t equivalent to 15 000 EJ; low-quality coal 4.3×10^{11} t or 1.9×10^{10} J/t unit energy equivalent to 8200 EJ [4,5,7]. The annual energy consumption worldwide was 283 EJ in 1980, 347 EJ in 1990, 400 EJ in 2000, 511 EJ in 1994, and 590 EJ in 2025. This rate is expected be increased at 607 EJ in the year of 2020, 702 EJ in 2030, 855 EJ in 2040, and 988 EJ in 2050 [1,6,15]. In the year 2017 the total fossil energy consumption was 560 EJ where building sector alone consumed 224 EJ. This means if the current level of fossil fuel consumption continues, the total fossil fuel energy source will be run out in 65 years. Since the fossil fuel causing severe environmental disaster and also getting finite level rapidly, thus, clean and renewable energy source is an urgent demand for the sustainability of the Earth. Here, the solar radiation has been defined as a sustainable energy to implement in the building exterior skin by the process of photo physical reaction to act PV panel to produce the clean energy to satisfy it total energy demand without any outsource connection. The average solar radiation on the Earth's surface is 1366 W/m^2, commonly known as solar constant. The radius of earth is $(2/\pi) \times 107$ m and thus, the total solar radiation reaching the Earth is solar = $1366 \times (4/\pi) \times 1014 \sim = 1.73 \times 10^{17}$W [7,35]. There are 86 400 s a day, with an average of 365.2422 days a year. Total annual solar radiation energy per year = $1.73 \times 1017 \times 86\,400 \times 365.2422 = 5.46 \times 1024$ J, Equivalent to 5,460,000 EJ/year (Fig. 1). The world energy consumption in 2017 was 5.60×10^{20}

* Address: Department of Civil and Urban Engineering, New York University, 6 Metrotech Center, Brooklyn, NY 11201, USA.
E-mail address: faruque55@aol.com.

https://doi.org/10.1016/j.applthermaleng.2018.05.085
Received 8 March 2018; Received in revised form 21 April 2018; Accepted 20 May 2018
Available online 31 May 2018
1359-4311/ © 2018 Elsevier Ltd. All rights reserved.

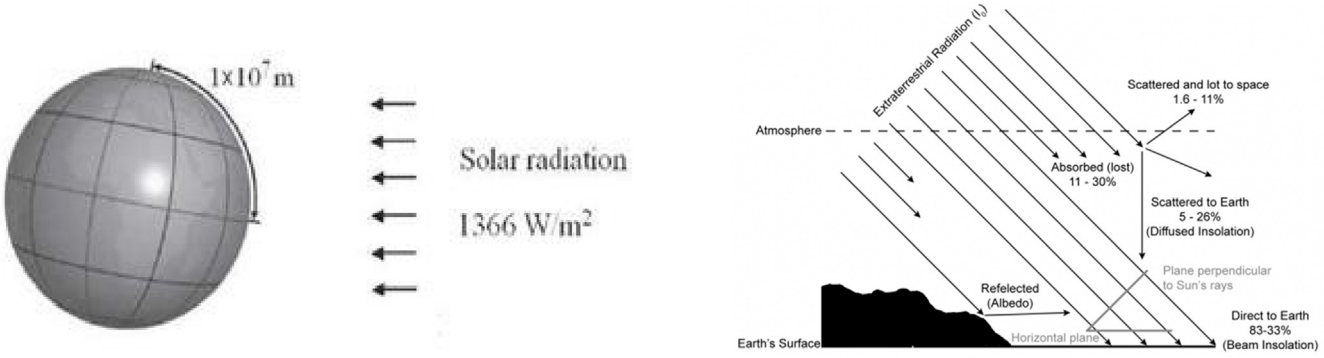

Fig. 1. (a) Shows the yearly solar irradiance arrives on surface of Earth. The mean solar energy on the Earth is 1366 W/m^2 respectively. The length of the meridian of Earth is 10 000 000 m. The total solar irradiance that arrives at the surface of Earth per year is 5,460 000 EJ calculatively (b) The effect of the atmosphere on the solar radiation reaching the Earth's Surface.

J = 560 EJ, of which nearly 40% was spent by building sector. Only 0.01% of the solar energy reaching the earth can meet the global energy demand where building sector can play vital role to harvest solar energy by its exterior skin to fulfill the mission of clean energy technology for the sustainability of the mother Earth.

In the past several decades, huge research has been performed on solar energy and its supply technology to the national grid for commercial application as the source of alternative energy technology [8,9,13,14]. Shi el al. showed that solar energy can be harvested by installing massive solar panel in a particular places tropical or subtropical area and then supply to the national grid as a source of sustainable energy technology [47]. Gleyzes et al. suggested an advanced mechanism of solar panel by the application of graphene silicon surface can have the ability to maximum 30% efficiency to capture the solar energy to convert into clean energy [12]. Reinhard, et al. shows that the breakdown of photon energy and its application by quantum machines into a PV panel can produce tremendous amount of clean energy [41]. All these research findings are indeed interesting, but these technologies required additional place and technology, supply mechanism to utilize the solar energy, and none of these investigations revealed that this solar energy can be utilized directly by the building itself by using its exterior curtainwall to act as the PV panel to produce energy. In this research, therefore, an innovative technology has been proposed to design all buildings to have at least 25% of the exterior is curtain walls to be used as the photovoltaic (PV) panel to capture the solar radiation and then convert it into clean energy to meet the total energy demand for a building.

2. Methods and materials

The building is proposed to design of which 25% of the exterior curtain walls to be built with solar panels. Prior to that this solar panel acting curtain wall skin must be determined the factor involved angle, latitude, longitude, and coordinate transformation in a Cartesian coordinate system to ensure that the maximum solar thermal radiation can be captured by the panel (Fig. 2). Considering angle, acting solar panel need to be designed for the effect of latitude and module tilt on the solar radiation received throughout the year and the module is to be facing south in the northern hemisphere and north in the southern hemisphere [10,17,18]. Cartesian coordinates for the horizon system need to be used accordingly where south should be x, west should be y, and the zenith should be z [11,12,52]. These positions of the celestial body are to be determined by two angles, height h and azimuth angle A; Cartesian coordinates for the equatorial system of z'-axis points to the North Pole, east-west axis y'-axis and the x'-axis are be in perpendicular to the both director. Then the position of the celestial body is to be determined by declination δ and hour angle ω, refer to figure in the preceding texts.

Since the light is an electromagnetic wave which is produced when an electric charge vibrates due to a hot object, thus, acting PV panel installation must follow the longitude and latitude and, polar coordinates and three dimensions axis (x,y,z) to get maximum sunlight obtainable on the building whole year considering the Stefan–Boltzman laws. The clarification of Stefan–Boltzman laws is that the electromagnetic waves follow the equal-partition radiation intensity once it emits on the plane of the PV panel [60,65].

Once the angles and Cartesian coordinates of the solar panel is determined, then the panel wiring diagram is focused on ensuring that the photovoltaic DC current can transmit into AC current at high efficient [21,34]. Thus, two of the Kyocera plates are mounted on aluminum bars to carry light from photovoltaic modules DC and then multiplies into the short-circuit current by 125% and uses this value for all 80% efficiency and then get AC current 125% of the continuous flow of the current by using three-parallel circuit.

Thereafter, number of parameters of the current-voltage (*I-V*) characteristic are necessarily be explained considering two/single diode equivalent circuit model of the PV cell [33,36,45]. Subsequently, the photovoltaic array at various parameters (*voltage proliferation, transformation rate, an PVVI curves)* and least control strategy are being used to confirm the active electricity production (I_{v+}) from solar energy to the utilization it by the building itself (see Fig. 3).

The next step is to determine the photovoltaic current production by I_{pv} calculation from the model of one diode (Fig. 5a), considering *I-V-R* relationship (Fig. 5b), and using the illumination received by the photovoltaic array to convert from DC to AC and then use for domestic energy and low voltage current demand (Fig. 5c).

Since the solar thermal energy is taken by the photophysical reaction of photovoltaic panel (PV) which is a continuum flow of photons into the PV panel, thus, it is necessary to determine the excellent photophysical reaction into the curtain wall acting PV panel. For this, it is essential to clarify solar thermal conductivity, solar cell anti-reflective coatings by analyzing quantum electrodynamics, the most effective fields in modern physics to capture much more solar energy [16,19,20]. Subsequently, classical statistical physics has been used to determine the radiation energy density of inner surface on its (curtain wall) considering the electromagnetic wave and Maxwell-Boltzmann constant statistics (Fig. 4). Therefore, a mathematical model of photovoltaic dynamic, in this research, has been developed to capture maximum solar energy by the acting PV panel of building exterior skin curtain wall where the following equation, calculates the energy output of a photovoltaic (PV) cell:

$$P_{pv} = \eta_{pvg} A_{pvg} G_t \tag{1}$$

In this equation, η_{pvg} refers to the PV-generation efficiency, A_{pvg} refers to the PV generator area (m^2), and G_t refers to the solar radiation in a titled module plane (W/m^2). η_{pvg} can be further defined as:

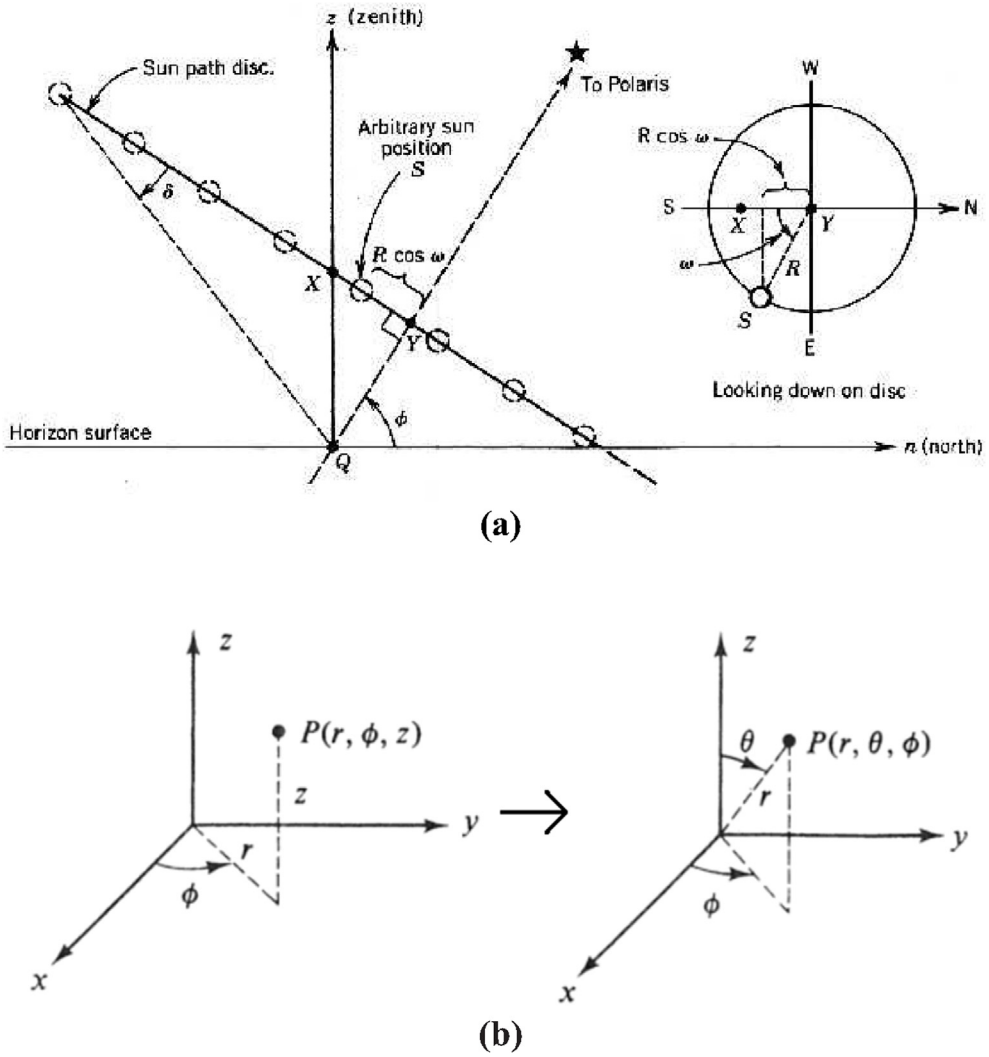

Fig. 2. (a) Photovoltaic (PV) panel angle has been calculated in consideration of the impact of latitude and mode tilt on the solar energy received within the year, (b) The Cartesian coordinate has been utilized for the horizon clarification considering use the conventions where south is *x*, west is *y*, and *z* the position of a celestial body and it is determined by two angles of the equatorial systems.

$$\eta_{pvg} = \eta_r \eta_{pc}[1-\beta(T_c - T_{cref})] \tag{2}$$

η_{pc} refers to the power conditioning efficiency, when MPPT applied, it is equal to 1; β refers to temperature coefficient (0.004–0.006 per °C); η_r refers to the reference module efficiency; and T_{cref} refers to the reference cell temperature in °C. The reference cell temperature (Tc_{ref}) can be obtained from the relation below:

$$T_c = T_a + \left(\frac{NOCT-20}{800}\right)G_t \tag{3}$$

T_a refers to the ambient temperature in °C, G_t refers to the solar irradiance in a tilted module plane (W/m^2), and NOCT refers to the standard operating cell temperature in Celsius (°C) degree. The total irradiance in the solar cell, considering both standard and diffuse solar irradiance, can be estimated by the following equation:

$$I_t = I_b R_b + I_d R_d + (I_b + I_d) R_r \tag{4}$$

The solar cells, which is essentially a P-N junction semiconductor able to produce electricity via the PV effect, which is interconnected in a series–parallel configuration to form a photovoltaic (PV) cell [53,58,59]. Besides, to improve the efficiency of the resulting photovoltaic (PV), graphene is integrated into the PV module [46,47,54].

Using a standard single diode, as depicted in Fig. 2, for a cell with N_s series-connected arrays and N_p parallel-connected arrays, the cell current must be related to the cell voltage as

$$I = N_p\left[I_{ph} - I_{rs}\left[\exp\left(\frac{q(V+IR_s)}{AKTN_s} - 1\right)\right]\right] \tag{5}$$

where

$$I_{rs} = I_{rr}\left(\frac{T}{T_r}\right)^3 exp\left[\frac{E_G}{AK}\left(\frac{1}{T_r} - \frac{1}{T}\right)\right] \tag{6}$$

In Eqs. (5) and (6), q refers to the electron charge (1.6×10^{-9}C), K refers to Boltzmann's constant, A refers to the diode idealist factor, and T refers to the cell temperature (K). I_{rs} refers to the cell reverse saturation current at T, T_r refers to the cell referred temperature, I_{rr} refers to the reverse saturation current at T_r, and E_G refers to the band gap energy of the semiconductor used in the cell. The photo current I_{ph} varies with the cell's temperature and radiation as follows:

$$I_{ph} = \left[I_{SCR} + k_i(T - T_r)\frac{S}{100}\right] \tag{7}$$

I_{SCR} refers to the cell short-circuit current at the reference temperature and irradiance, k_i refers to the short-circuit current temperature coefficient, and S refers to the solar irradiance (mW/cm^2). The *I-V* characteristics of the photovoltaic (PV) cell can be derived using a single-diode model which includes an additional shunt resistance concurrent

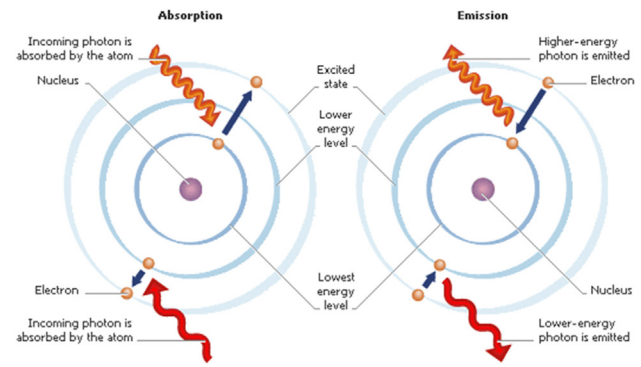

4(1)

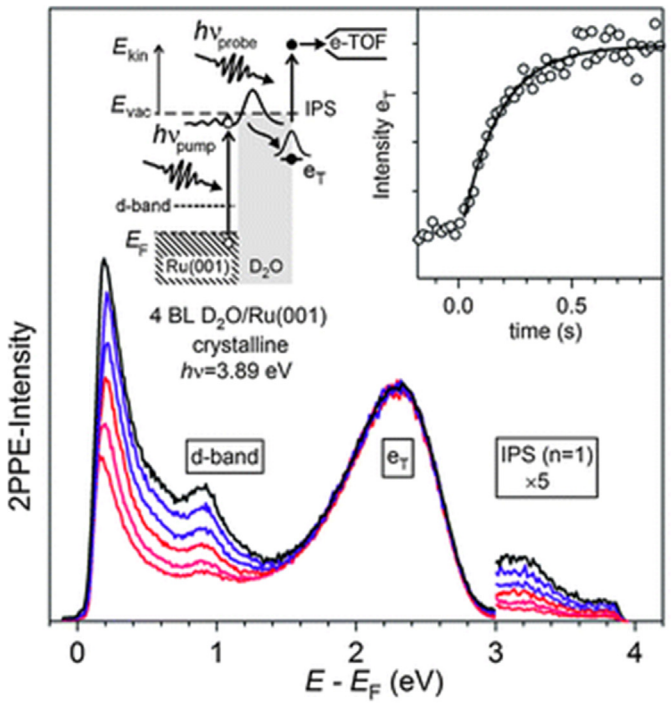

4 (2)

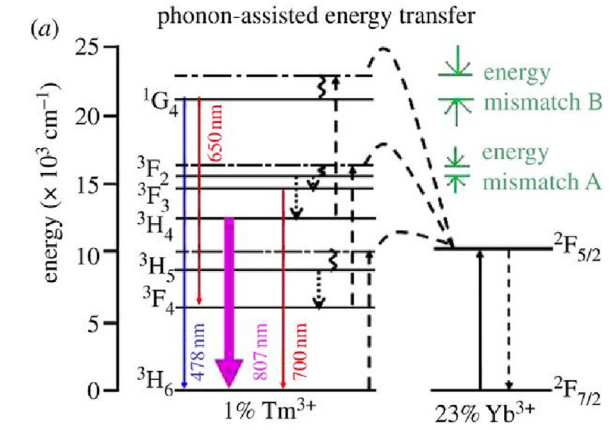

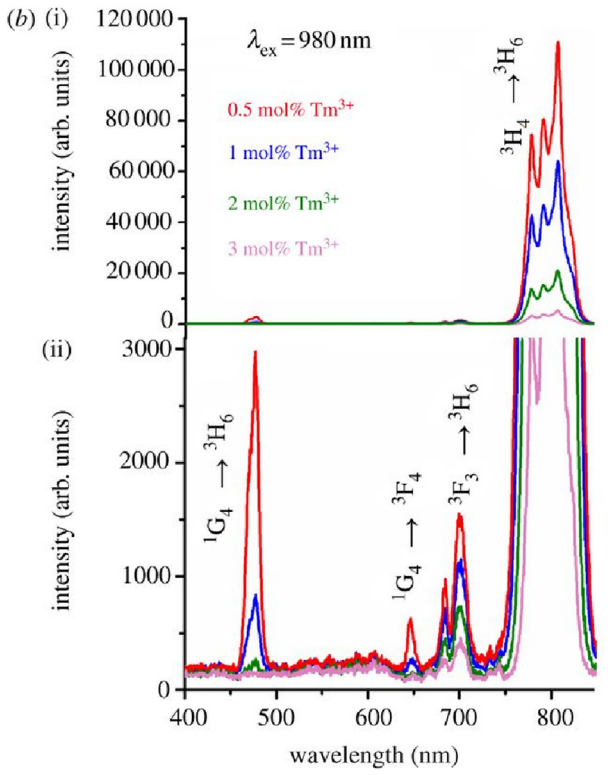

4(3)

Fig. 3. Diagram of PV system model, (1) The module photon absorption and emission reaction mechanism once solar irradiance are on the photovoltaic mode, (b) Solar intensity rate, (3) (*a*) the irradiation energy at 980 nm; solid arrows represent photon absorption or emission, dotted arrows represent multi-phonon relaxation, dashed arrows represent phonon assisted energy transfer, and wavy arrows represent energy mismatches. (*b*) (i) The up-conversion spectrum of UCNPs excited at 980 nm (90 mW), (ii) Vertical axis is magnified to show the details of the visible emission spectra.

with the optimal shunt diode model as follows:

$$I = I_{ph} - I_D \tag{8}$$

$$I = I_{ph} - I_0\left[\exp\left(\frac{q(V + R_s I)}{AKT} - 1\right) - \frac{V + R_s I}{R_{sh}}\right] \tag{9}$$

I_{ph} refers to the photo current (A), I_D refers to the diode current (A), I_0 refers to the inverse saturation current (A), *A* refers to the diode constant, *q* refers to the charge of the electron (1.6×10^{-9}C), *K* refers to Boltzmann's constant, *T* refers to the cell temperature (°C), R_s refers to the series resistance (ohm), R_{sh} refers to the shunt resistance (Ohm), *I* refers to the cell current (A), and *V* refers to the cell voltage (V). The output current of the PV cell using the diode model can be described as follows:

$$I = I_{PV} - I_{D1} - I_{D2} - \left(\frac{V + IR_S}{R_{SH}}\right) \tag{10}$$

where

$$I_{D1} = I_{01}\left[\exp\left(\frac{V + IR_s}{a_1 V_{T1}}\right) - 1\right] \tag{11}$$

$$I_{D2} = I_{02}\left[\exp\left(\frac{V + IR_s}{a_2 V_{T2}}\right) - 1\right] \tag{12}$$

I_{01} and I_{02} are the reverse saturation currents of diode 1 and diode 2, respectively, and V_{T1} and V_{T2} are the thermal voltages of the respective diodes. The diode idealist constants are represented by a_1 and a_2. The simplified model of the photovoltaic (PV) system model is presented below:

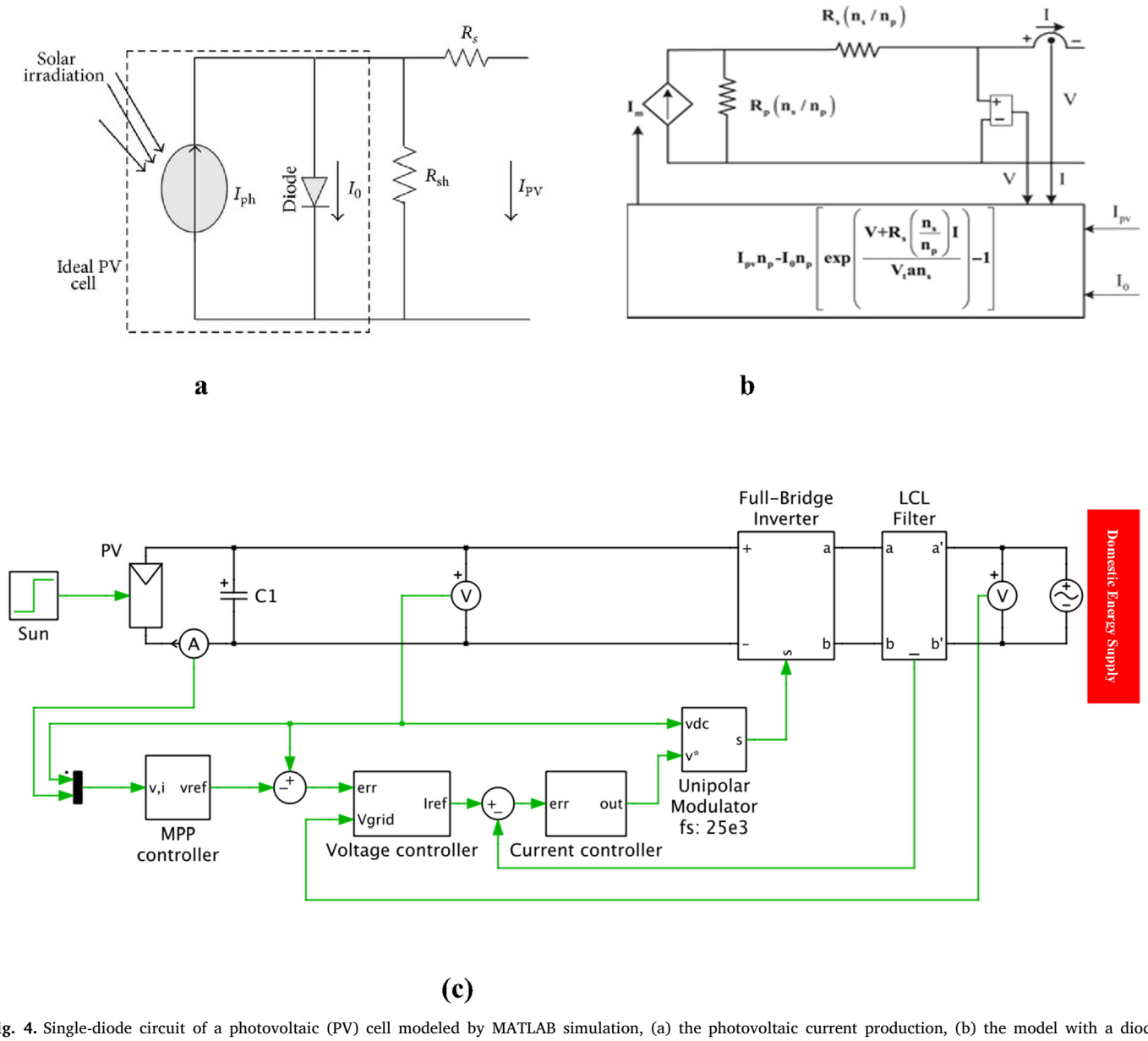

Fig. 4. Single-diode circuit of a photovoltaic (PV) cell modeled by MATLAB simulation, (a) the photovoltaic current production, (b) the model with a diode considering *I-V-R* relationship (c), the conversion process of DC to AC for the use of domestic energy and low voltage current for the building.

$$v_{oc} = \frac{V_{oc}}{cKT/q} \tag{13}$$

$$P_{max} = \frac{\frac{V_{oc}}{cKT/q} - \ln\left(\frac{V_{oc}}{cKT/q} + 0.72\right)}{\left(1 + \frac{V_{oc}}{nKT/q}\right)}\left(1 - \frac{V_{oc}}{\frac{V_{oc}}{I_{SC}}}\right)\left(\frac{V_{oc0}}{1 + \beta\ln\frac{G_0}{G}}\right)\left(\frac{T_o}{T}\right)^{y} I_{sc0}\left(\frac{G}{G_o}\right)^{a} \tag{14}$$

where ν_{oc} refers to the normalized value of the open-circuit voltage V_{oc} related to the thermal voltage $V_t = nkT/q$, K refers to Boltzmann's constant, n refers to the idealist factor ($1 < n < 2$), T refers to the temperature of the photovoltaic (PV) module in Kelvin, α refers to the factor responsible for all the non-linear effects on which the photocurrent depends, q refers to the electron charge, γ refers to the factor representing all the non-linear temperature-voltage effects, while β refers to a photovoltaic (PV) module technology-specific dimensionless coefficient. Eq. (14) only represents the maximum energy output of a single photovoltaic (PV) module while a real system consists of several photovoltaic (PV) modules connected in series and in parallel. Therefore, the equation of total power output for an array with N_s cells connected in series and N_p cells connected in parallel with power P_M for each module would be for PV panel

$$P_{array} = N_s N_p P_M \tag{15}$$

Naturally the movement of photon flux applied to the solar panel will be activated by the photo-physical reactions to deliver energy level charges [24,31]. Since the energy density of the solar radiation considering the photon wave frequency has been modeled by using the classical statistical physics in Fig. 7a, thus, the maximum solar energy formation considering a single photon excitation at the rate of 1.4 eV with an energy value of 27.77 MW/m^2 eV has been determined in Fig. 6b.

3. Results and discussion

The result of the PV model is determined by the I-V equation of PV cells in the single-diode mode. The I-V relationship equation in the PV panel can be expressed as

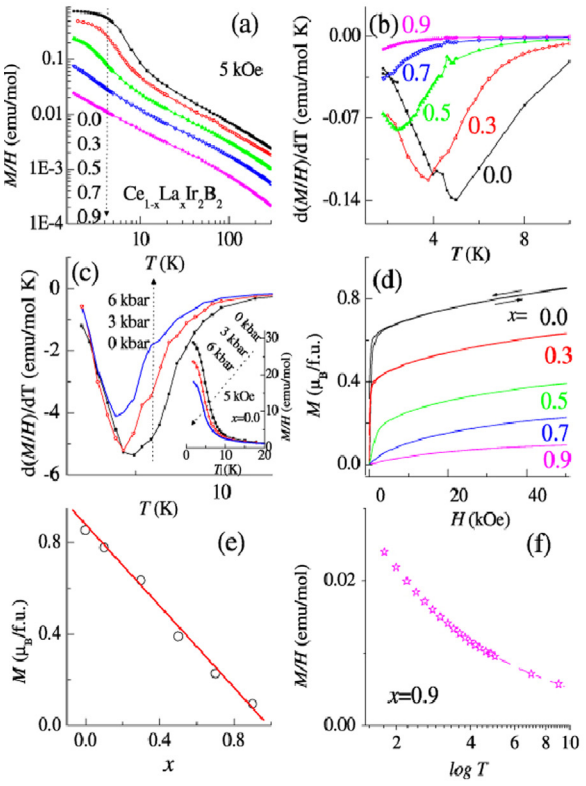

Figure 5 (1)

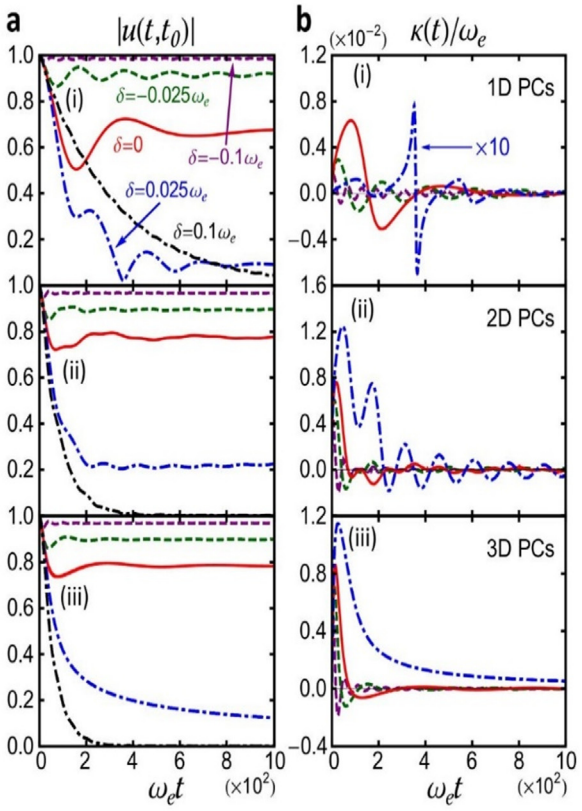

Figure 5 (2)

Fig. 5. (1) Photonic thermal activation mechanism in various PB parameters, (2) Dynamic photons emission in PV cells. (a) shows the charge generation in the PB area $\langle a(t)\rangle = 5u(t, t_0)\langle a(t_0)\rangle$, (b) demonstrates the dynamic photon emission rate k(t), plotted for (i) 1D, (ii) 2D and (iii) 3D areal field into the PV cells [22,23].

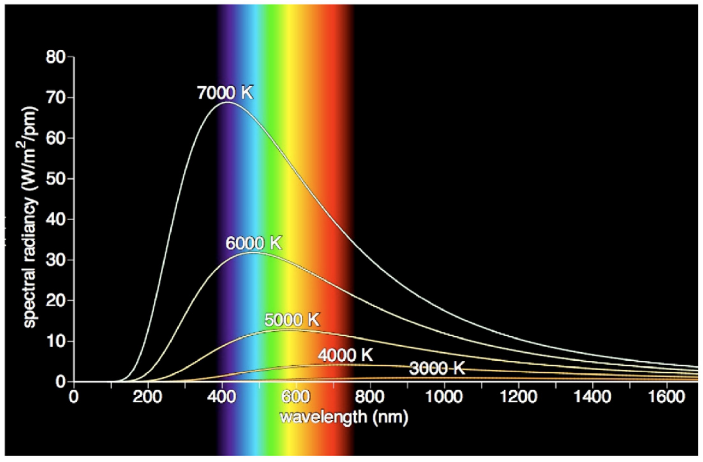

(a)

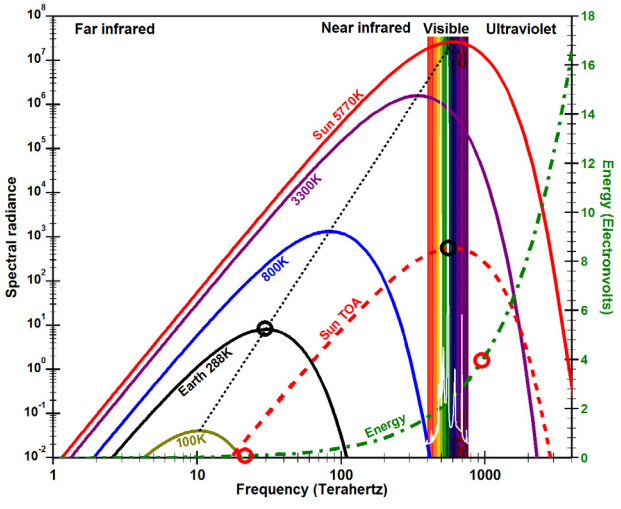

(b)

Fig. 6. The thermal energy density of the solar radiation frequencies shown by the classical statistical physics and the figure depicted the solar radiation in various temperature (a) The spectral irradiance of the light in difference wavelength, (b) The radiation in difference frequencies at different temperatures where the maximum irradiance by sun nearly at 5800 K (actual 5770 K) power is equivalent to 6.31×10^7(W/m^2); peak E is 1.410 (eV); peak λ is 0.88 (μm); peak μ is 2.81×10^7(W/m^2 eV).

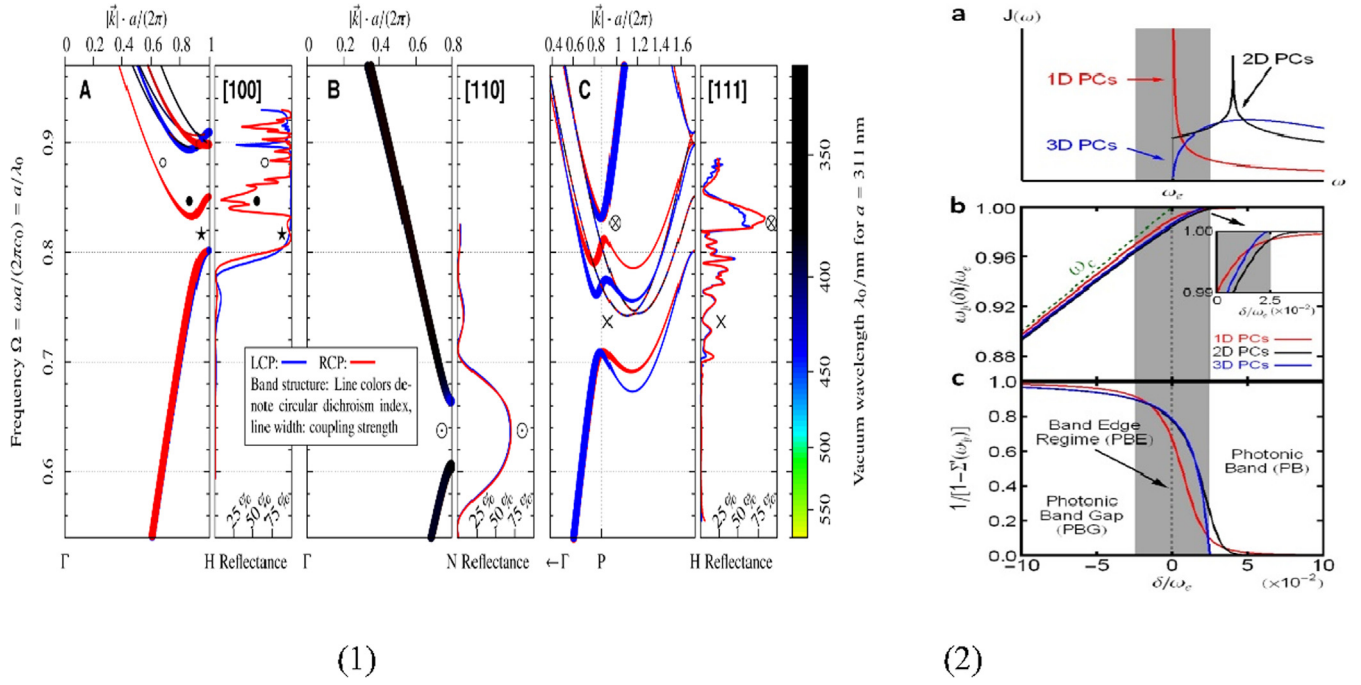

Fig. 7. (1) Photonic thermal energy conversion modes. 2(a) Unit area versus frequency at various DOSs in 1D, 2D, and 3D glazing wall skins. 2(b) Photonic modes of frequencies for functional tuning. 2(c) Photonic modes of magnitudes to release the energy calculated by Eq. (2). The photonic modes depict the crossover into the glazing wall skin in 1D and 2D. In the complex 3D transitional state, they depict the crossover into the PV cell once the point break frequency *vc* transforms from a PBG area to a photonic band (PB) area [55,70].

$$I = IL - IO\left\{exp^{[\frac{q(V+I_{RS})}{AkTc}]} - 1\right\} - \frac{(V + I_{RS})}{R_{Sh}} \tag{16}$$

I_L represents the photon generating current, *IO* represents the saturated current in the diode, R_s represent resistance in a series, A represents the diode passive function, k ($= 1.38 \times 10^{-23}\,W/m^2K$) represents Boltzmann's constant, q ($=1.6 \times 10^{-19}\,C$) represents the charge amplitude of an electron, and T_C represents the functional cell temperature. Subsequently, the I-q relationship in the PV cells varies owing to the diode current and/or saturation current, which can be expressed as [25,32].

$$I_O = I_{RS}\left(\frac{T_C}{T_{ref}}\right)^3 \exp[\frac{qEG(\frac{1}{T_{ref}} - \frac{1}{T_C})}{KA}] \tag{17}$$

where I_{RS} represents the saturated current considering the functional temperature and solar irradiance and *qEG* represents the band-gap energy into the silicon and graphene PV cell considering the normal, normalized, and perfect modes.

Considering a PV module, the I-V equation, apart from the I-V curve, is a conjunction of I-V curves among all cells of the PV panel. Therefore, the equation can be rewritten as follows to determine the V-R relationship:

$$V = -IR_s + K\log[\frac{I_L - I + I_O}{I_O}] \tag{18}$$

Here, K is as a constant ($=\frac{AkT}{q}$) and I_{mo} and V_{mo} are the current and voltage in the PV panel. Therefore, the relationship between I_{mo} and V_{mo} shall be same as the PV cell I-V relationship:

$$V_{mo} = -I_{mo}R_{Smo} + K_{mo}\log(\frac{I_{Lmo} - I_{mo} + I_{Omo}}{I_{Omo}}) \tag{19}$$

where I_{Lmo} represents the photon-generated current, I_{Omo} represents the saturated current into the diode, R_{smo} represent the resistance in series, and K_{mo} represents the factorial constant. Once all non-series (NS) cells are interconnected in series, then the series resistance shall be counted as the summation of each cell series resistance $R_{smo} = N_S \times R_S$, and the constant factor can express as $K_{mo} = N_S \times K$. There is a certain amount of current flow into the series connected cells; thus, the current flow in Eq. (5) remains the same in each component, i.e., $I_{omo} = I_o$ and $I_{Lmo} = I_L$. Thus, the module I_{mo}-V_{mo} equation for the N_S series of connected cells will be written as

$$V_{mo} = -I_{mo}N_S R_S + N_S K\log(\frac{I_L - I_{mo} + I_o}{I_o}) \tag{20}$$

Similarly, the current–voltage calculation can be rewritten for the parallel connection once all N_P cells are connected in parallel mode and can be expressed as follows [61,62,71]:

$$V_{mo} = -I_{mo}\frac{Rs}{Np} + K\log(\frac{N_{sh}I_L - I_{mo} + N_p I_o}{N_p I_o}) \tag{21}$$

Because the photon-generated current primarily will depend on the solar irradiance and relativistic temperature conditions of the PV panel, the current can be calculated using the following equation:

$$I_L = G[I_{SC} + K_I(T_C - T_{ref})] * V_{mo} \tag{22}$$

where I_{sc} represents PV current at 25 °C and KW/m^2, K_I represents the relativistic PV panel coefficient factor, T_{ref} represents the PV panel's functional temperature, and G represent the solar energy in KW/m^2.

4. Conversion of electricity

To convert solar thermal energy into electricity, a single-diode circuit has been used consisting of a small disk of semiconductor attached by wire to a circuit consisting of a positive and a negative film of silicon placed under a thin slice of glass and attached to graphene, using a building's exterior curtain wall skin. Necessarily, the PV panel shall have an *open circuit point*, where the current and voltage is at the maximum, open circuit voltage Voc, and the *maximum power point* can be clarified using the maximum current and voltage calculation immediately upon capturing the non-equilibrium photons [26,44,48]. The power delivered by a PV panel will thus have the capability to attain a

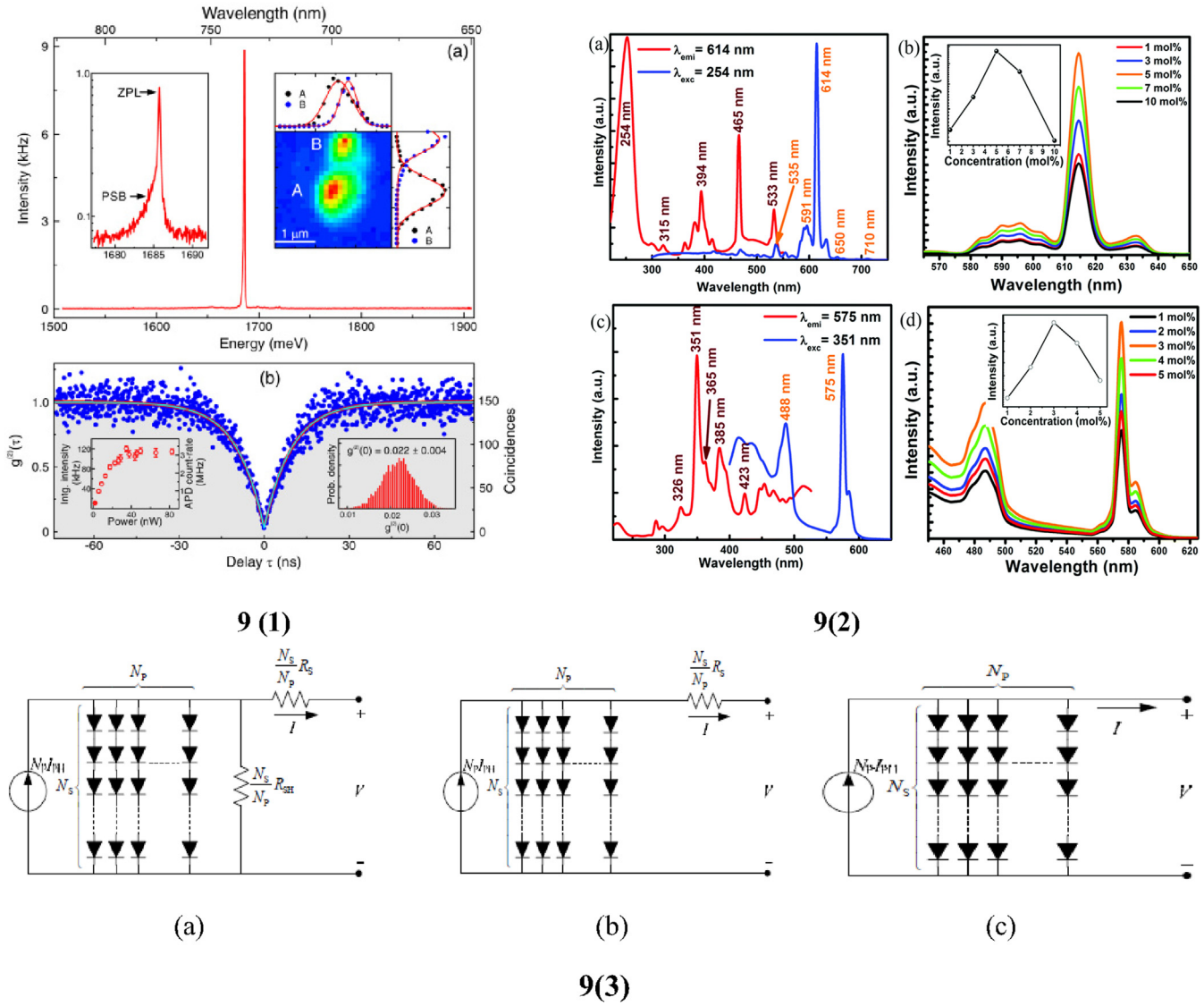

Fig. 8. Solar cell current-voltage characteristic features for conceptual function of (1) net optimal solar energy production intensity with respect the delay of coincidental factor and (2) intensity of solar energy production in various wavelength, (3) the current-voltage module of the current source near the short circuit point and as a voltage source in the vicinity of the open circuit point at the condition of the PV module is (a) normal, (b) normalized, and (c) perfect modes.

Table 1
Design and Construction Cost of the Curtain Wall Acting Solar Panel for Energy Production of a 10 Stories Building.

List of Component	Materials Cost	Labor Cost	Equipment Cost	GC & OH Cost	Total Cost
Acting Solar Panel	$10,000	$5000	$2500	$3500	$21,000
Instrumentation	$2000	$1000	$2000	$1000	$6000
Electrical, and Mechanical Control	$2500	$1000	$1000	$900	$5400
Supply for 30 Years cost at $0.05/kWh for monthly 4000 kWh for 100 people					$72,000
				Total Cost	$104,400

Table 1: The estimates is (1 m^2 each solar panel and total 1195 panels) prepared by confirming recent (June 2017) cost of material for selective manufacturer and labor rate added in accordance with international of union specified trade workers Considering US location. The equipment rental cost is calculated as current rental market in conjunction with the standard practice of construction of the production rate.

maximum value at the points (I_{mp},V_{mp}) [27,28,42]. It is confirmed by the PV panel's capability of such current-voltage flow to get net energy production by the PV panel by analysing circuit models of the PV module (a) normal, (b) normalized, and (c) perfect modes where perfect modes are the best option.

To establish a connection between the number of light-quanta solar energy by steady state, the intensity of solar irradiance is considered to convert it into electricity energy by PV panel [66,67,69]. The number of stationary states of light-quanta is a certain type of polarization whose frequency is in the range of ν_r to $\nu_r + d\nu_r$ [40,41,43]. From there maximum solar radiation it can be achieved at 1.4 eV with an energy value of 27. 77 mW/m^2 eV based on an average of 5 h solar irradiance harvesting in a day peak levels, which is the equivalent of 27,770 kW / year or 7.6 kW / day energy [29,68]. Due to physical principles, there are losses in the conversion of solar energy into DC power and converting direct current into alternating current (AC). This ratio of AC to

DC is called “derating factor ', which is typically 0.8 [30,63,64]. Thus, the surface texture of selective solar metal is excellent in energy conversation [33,34,62], since the current net conversion by solar panels is 125% higher level with an efficiency of 80% [8,13,14] of solar panels which means that (27,770 × 1.25 × 0.8) = 27,770 kW/year or 7.6 kW/day. Energy remains equal to the solar initially what was before the introduction to the solar panel. Necessarily, the maximum solar irradiance is depicted 1.4 eV with an energy value of 27.77 mW/m^2 eV in Fig. 8 per year in an average of five hours a day maximum levels for 365 days referents by panel Solar and black body [37,56,71]. A standard residential house requires average 6 kW/day [50,57,61]. Since the produced energy is equivalent to 27,770 kW/year or 7.6 kW/day, which in fact will meet the energy demand for a residential house required 6 kW/day by using only one solar panel 1 m^2. The average energy consumption rate monthly of commercial office or buildings is about 10,000 kW/day for a foot printing 32 m x 31 m with 30 m (10 floors), respectively [38,39,49]. In calculation of a building is an average of 32 m × 31 m footprint with a height of 30 m, total installed 1 m^2 PV panels requires 1195 units (945 + 250) with the capacity of 7.6 kW/unit energy production can provide total energy × 1195 = 9082 kW/day to meet the daily energy demand of about10,000 kW/day for a commercial office or building (see Table 1).

4.1. Savings on energy Cost

On the other hand, the net cost for 30 years energy purchase from a traditional utility sources for a standard industry (100 people capacity) at 0.12/kWh of 4000 kWh per month is (30 × 12 × 4000 × 0.12) $172,800. This difference between traditional energy use and curtain wall assisted PV panel energy production clearly indicate the cost saving of $68,400 once curtain wall assisted PV panel is used as the energy source.

5. Conclusions

In recent decades, concern about the deadly risks of greenhouse gases (GHGs) has been growing due to their level of accumulation in the atmosphere and the adverse impact on Earth. Given that conventional energy consumption is the final factor that leads to environmental perplexity and climate change, the intelligent deployment of solar energy, in effect, for a better methodological application to mitigate global environmental perplexity and climate changes is an urgent demand. In addition, the limited nature of the fossil fuel reserve poses a serious challenge for future energy supply as the consumption of fossil fuels will end in the next 65 years. In this study, it is therefore, proposed to ensure an economical, reliable sustainable energy technology to meet the future energy demand which is also climate-friendly. Simply capturing solar thermal energy using exterior curtain wall demonstrated, in this research shall indeed be the innovative technology to meet the total energy demand for the building sector and contribute with the quota to mitigate the global energy needs. Therefore, application of this sustainable energy technology is very much computational that need to be encouraged globally for the maximum utilization of solar energy harvesting by building sector to secure a sustainable and environmentally friendly earth.

Acknowledgments

This research was supported by Green Globe Technology, Inc. under grant RD-02018-03 for building a better environment. Any findings, predictions, and conclusions described in this article are solely those of the authors, who confirm that the article has no conflicts of interest for publication in a suitable journal.

References

[1] D.K. Armani, T.J. Kippenberg, S.M. Spillane, K.J. Vahala, Ultra-high-Q toroid microcavity on a chip, Nature 421 (2003) 925.
[2] N. Artemyev, U.D. Jentschura, V.G. Serbo, A. Surzhykov, Strong electromagnetic field EFFECTS in ultra-relativistic heavy-ion collisions, Eur. Phys. J. C 72 (2012) 1935.
[3] K.M. Birnbaum, et al., Photon blockade in an optical cavity with one trapped atom, Nature 436 (2005) 87–90.
[4] K. Busch, G. von Freymann, S. Linden, S.F. Mingaleev, L. Tkeshelashvili, M. Wegener, Periodic nanostructures for photonics, Phys. Rep. 444 (2007) 101.
[5] D.E. Chang, A.S. Sørensen, E.A. Demler, M.D. Lukin, A single-photon transistor using nanoscale surface plasmons, Nat. Phys. 3 (2007) 807–812.
[6] J. Chen, C. Wang, R. Zhang, J. Xiao, Multiple plasmon-induced transparencies in coupled-resonator systems, Opt. Lett. 37 (2012) 5133–5135.
[7] M. Cheng, Y. Song, Fano resonance analysis in a pair of semiconductor quantum dots coupling to a metal nanowire, Opt. Lett. 37 (2012) 978–980.
[8] B. Dayan, et al., A photon turnstile dynamically regulated by one atom, Science 319 (2008) 1062–1065.
[9] J.S. Douglas, H. Habibian, C. Hung, A. Gorshkov, H. Kimble, D. Chang, Quantum many-body models with cold atoms coupled to photonic crystals, Nat. Photon. (2015).
[10] J. Eichler, Th. Stöhlker, Radiative electron capture in relativistic ion-atom collisions and the photoelectric effect in hydrogen-like high-Z systems, Phys. Rep. 439 (2007) 1.
[11] D. Englund, et al., Resonant excitation of a quantum dot strongly coupled to a photonic crystal nanocavity, Phys. Rev. Lett. 104 (2010) 073904.
[12] S. Gleyzes, et al., Quantum jumps of light recording the birth and death of a photon in a cavity, Nature 446 (2007) 297.
[13] R.J. Gould, Pair Production in Photon-Photon Collisions, Phys. Rev., 03/1967.
[14] C. Guerlin, et al., Progressive field-state collapse and quantum non-demolition photon counting, Nature 448 (2007) 889.
[15] N. Gupta, S.P. Singh, S.P. Dubey, D.K. Palwalia, Fuzzy logic controlled three-phase three-wired shunt active power filter for power quality improvement, (2011), in: International Review of Electrical Engineering (IREE), 6 (3), pp. 1118–1129.
[16] Z. Han, S.I. Bozhevolnyi, Plasmon-induced transparency with detuned ultracompact Fabry-Pérot resonators in integrated plasmonic devices, Opt. Exp. 19 (2011) 3251–3257.
[17] Md. Hossain, Faruque, Solar energy integration into advanced building design for meeting energy demand, Int. J. Energy Res. 40 (2016) 1293–1300.
[18] Md. Faruque Hossain, Design and construction of ultra-relativistic collision pv panel and its application into building sector to mitigate total energy demand. J. Build. Eng. 10.1016/j.jobe.2016. 12.005.
[19] Md. Faruque Hossain, Green science: independent building technology to mitigate energy, environment, and climate change. Renew. Sustain. Energy Rev. 10.1016/j.rser.2017.01.136.
[20] Md. Hossain, Faruque, Green science: advanced building design technology to mitigate energy and environment, Renew. Sustainable Energy Reviews. 81 (2) (2018) 3051–3060.
[21] Md. Hossain, Faruque, Photonic thermal energy control to naturally cool and heat the building, Adv. Therm. Eng. 131 (2018) 576–586.
[22] Md. Hossain, Faruque, Transforming dark photon into sustainable energy, Int. J. Energy Environ. Eng. (2018), http://dx.doi.org/10.1007/s40095-017-0257-1.
[23] J.F. Huang, T. Shi, C.P. Sun, F. Nori, Controlling single-photon transport in waveguides with finite cross section, Phys. Rev. A 88 (2013) 013836.
[24] Y. Huang, C. Min, G. Veronis, Subwavelength slow-light waveguides based on a plasmonic analogue of electromagnetically induced transparency, Appl. Phys. Lett. 99 (2011) 143117.
[25] U. Jentschura, K. Hencken, V. Serbo, Revisiting unitarity corrections for electromagnetic processes in collisions of relativistic nuclei, Eur. Phys. J. C 58 (2) (2008) 281–289.
[26] J.D. Joannopoulos, P.R. Villeneuve, S. Fan, Photnic crystals: putting a new twist on light, Nature 386 (1997) 143.
[27] Kai Hencken, Transverse momentum distribution of vector mesons produced in ultraperipheral relativistic heavy ion collisions, Phys. Rev. Lett., 01/2006.
[28] S.A. Klein, Calculation of flat-plate collector loss coefficients, Sol. Energy 17 (1975) 79–80.
[29] A.G. Kofman, G. Kurizki, B. Sherman, Spontaneous and induced atomic decay in photonic band structures, J. Mod. Opt. 41 (1994) 353.
[30] P. Kolchin, R.F. Oulton, X. Zhang, Nonlinear quantum optics in a waveguide: Distinct single photons strongly interacting at the single atom level, Phys. Rev. Lett. 106 (2011) 113601.
[31] C. Lang, et al., Observation of resonant photon blockade at microwave frequencies using correlation function measurements, Phys. Rev. Lett. 106 (2011) 243601.
[32] C.U. Lei, W.M. Zhang, A quantum photonic dissipative transport theory, Ann. Phys. 327 (2012) 1408.
[33] Q. Li, D.Z. Xu, C.Y. Cai, C.P. Sun, Recoil effects of a motional scatterer on single-photon scattering in one dimension, Scient. Rep., 2013.
[34] J.Q. Liao, C.K. Law, Correlated two-photon scattering in cavity optomechanics, Phys. Rev. A 87 (2013) 043809.
[35] J.Q. Liao, C.K. Law, Correlated two-photon transport in a one-dimensional waveguide side-coupled to a nonlinear cavity, Phys. Rev. A 82 (2010) 053836.
[36] P. Lo, H. Xiong, W. Zhang, Breakdown of Bose-Einstein distribution in photonic crystals, Scient. Rep., 2015.
[37] P. Longo, P. Schmitteckert, K. Busch, Few-photon transport in low-dimensional

systems, Phys. Rev. A 83 (2011) 063828.
[38] X. Lü, W. Zhang, S. Ashhab, Y. Wu, F. Nori, Quantum-criticality-induced strong Kerr nonlinearities in optomechanical systems, Scient. Rep., 2013.
[39] B. Najjari, A. Voitkiv, A. Artemyev, A. Surzhykov, Simultaneous electron capture and bound-free pair production in relativistic collisions of heavy nuclei with atoms, Phys. Rev. A 80 (2009) 012701.
[40] D. O'Shea, C. Junge, J. Volz, A. Rauschenbeutel, Fiber-optical switch controlled by a single atom, Phys. Rev. Lett. 111 (2013) 193601.
[41] A. Reinhard, Strongly correlated photons on a chip, Nat. Photon. (2011).
[42] D. Roy, Two-photon scattering of a tightly focused weak light beam from a small atomic ensemble: An optical probe to detect atomic level structures, Phys. Rev. A 87 (2013) 063819.
[43] Alberto Ruiz. Partial recovery of a potential from backscattering data, Communications in Partial Differential Equations, Springer Tracts in Modern Physics, 2014.
[44] C. Sánchez Muñoz, F. Laussy, E. Valle, C. Tejedor, A. González-Tudela, Filtering multiphoton emission from state-of-the-art cavity quantum electrodynamics, Optica 5 (1) (2018) 14–26.
[45] C. Sayrin, et al., Real-time quantum feedback prepares and stabilizes photon number states, Nature 477 (2011) 73.
[46] J.T. Shen, S. Fan, Strongly correlated two-photon transport in a one-dimensional waveguide coupled to a two-level system, Phys. Rev. Lett. 98 (2007) 153003.
[47] T. Shi, S. Fan, C.P. Sun, Two-photon transport in a waveguide coupled to a cavity in a two-level system, Phys. Rev. A 84 (2011) 063803.
[48] M.S. Tame, K.R. McEnery, Ş.K. Özdemir, J. Lee, S.A. Maier, M.S. Kim, Quantum plasmonics, Nat. Phys. (2013).
[49] M.W.Y. Tu, W.M. Zhang, Non-Markovian decoherence theory for a double- dot charge qubit, Phys. Rev. B 78 (2008) 235311.
[50] S.R. Valluri, U. Becker, N. Grün, W. Scheid, Relativistic collisions of highly-charged ions, J. Phys. B: At. Mol. Phys. 17 (1984) 4359.
[51] Y.F. Xiao, et al., Asymmetric Fano resonance analysis in indirectly coupled micro-resonators, Phys. Rev. A 82 (2010) 065804.
[52] W. Yan, H. Fan, Single-photon quantum router with multiple output ports, Scient. Rep., 2014.
[53] W. Yan, J. Huang, H. Fan, Tunable single-photon frequency conversion in a Sagnac interferometer, Scient. Rep., 2013.
[54] L. Yang, S. Wang, Q. Zeng, Z. Zhang, T. Pei, Y. Li, L. Peng, Efficient photovoltage multiplication in carbon nanotubes. Nat. Photon. (2011) 672–676.
[55] W.M. Zhang, P.Y. Lo, H.N. Xiong, M.W.Y. Tu, F. Nori, General non- markovian dynamics of open quantum systems, Phys. Rev. Lett. 109 (2012) 170402.
[56] Yuwen Wang, Yongyou Zhang, Qingyun Zhang, Bingsuo Zou, Udo Schwingenschlogl. Dynamics of single photon transport in a one-dimensional waveguide twopoint coupled with a Jaynes-Cummings system, Scient. Rep., 2016.
[57] Wei-Bin Yan, Jin-Feng Huang, Heng Fan, Tunable single-photon frequency conversion in a Sagnac interferometer, Scient. Rep., 2013.
[58] Wei-Bin Yan, Heng Fan, Single-photon quantum router with multiple output ports, Scient. Rep., 2014.
[59] G. Yu, A novel two-mode MPPT control algorithm based on comparative study of existing algorithms, Sol. Energy, 2004, 04.
[60] H.F. Beyer, T. Gassner, M. Trassinelli, R. Heß, U. Spillmann, D. Banaś, K.-H. Blumenhagen, F. Bosch, C. Brandau, W. Chen, Chr. Dimopoulou, E. Förster, R.E. Grisenti, A. Gumberidze, S. Hagmann, P.-M. Hillenbrand, P. Indelicato, P. Jagodzinski, T. Kämpfer, Chr. Kozhuharov, M. Lestinsky, D. Liesen, Yu A. Litvinov, R. Loetzsch, B. Manil, R. Märtin, F. Nolden, N. Petridis, M.S. Sanjari, K. S Schulze, M. Schwemlein, A. Simionovici, M. Steck, Th. Stöhlker, C.I. Szabo, S. Trotsenko, I. Uschmann, G. Weber, O. Wehrhan, N. Winckler, D.F.A Winters, N. Winters, E. Ziegler. Crystal optics for precision x-ray spectroscopy on highly charged ions—conception and proof, J. Phys. B Atom. Mol. Opt. Phys., 2015.
[61] Yu Zhu, Xiaoyong Hu, Hong Yang, Qihuang Gong, On-chip plasmon-induced transparency based on plasmonic coupled nanocavities, Scient. Rep., 2014.
[62] Jing Tang, Weidong Geng, and Xiulai Xu, Quantum interference induced photon blockade in a coupled single quantum dot-cavity system, Scient. Rep., 2015.
[63] Hiroyuki Okamoto, Kenzo Yamaguchi, Masanobu Haraguchi, Toshihiro Okamoto, Development of plasmonic racetrack resonators with a trench structure, Plasmon. Metall. Nanostruct. Their Opt. Propert. X, 2012.
[64] Andreas Kalb Reiserer, Norbert Rempe, Gerhard Ritter, Stephan, A quantum gate between a flying optical photon and a single trapped atom (RESEARCH: LETTER) (Report), Nature, April 10, 2014.
[65] Qiong Li, D.Z. Xu, C.Y. Cai, C.P. Sun, Recoil effects of a motional scatterer on single-photon scattering in one dimension, Scient. Rep, 2013.
[66] Marco T. Manzoni, Darrick E. Chang, James S. Douglas. Simulating quantum light propagation through atomic ensembles using matrix product states, Nat. Commun.
[67] Alexander V. Poshakinskiy, Alexander, N. Poddubny, Biexciton-mediated super-radiant photon blockade, Phys. Rev. A, 2016.
[68] W. Zhou, A novel model for photovoltaic array performance prediction, Appl. Energy, 2007, 12.
[69] H. Matteo Mariantoni, Radoslaw C. Wang, M. Lenander Bialczak, et al., Photon shell game in three-resonator circuit quantum electrodynamics, Nat. Phys. (2011).
[70] H. Rauh. Optical transmittance of photonic structures with linearly graded dielectric constituents, New J. Phys., 07/26/2010.
[71] Etienne Saloux, Alberto Teyssedou, Mikhaïl Sorin, Explicit model of photovoltaic panels to determine voltages and currents at the maximum power point, Sol. Energy (2011).